Luminosity thresholds of colored surfaces are determined by their heuristic upper-limit luminances in the visual system

Takuma Morimoto[1]*, Ai Numata[2], Kazuho Fukuda[3] and Keiji Uchikawa[4]

1: Department of Experimental Psychology, University of Oxford, Oxford, UK
2: Department of Information Processing, Tokyo Institute of Technology, Yokohama, Japan
3: Department of Information Design, Kogakuin University, Tokyo, Japan
4: Human Media Research Center, Kanagawa Institute of Technology, Atsugi, Japan

*Corresponding author: takuma.morimoto@psy.ox.ac.uk
Address: New Radcliffe House, Radcliffe Observatory Quarter, Woodstock Road, Oxford OX2 6GG

Keywords: Luminosity threshold, Color vision, Optimal color

Abstract

Some objects in the real world themselves emit a light, and we typically have a fairly good idea as to whether a given object is self-luminous or illuminated by a light source. However, it is not well understood how our visual system makes this judgement. This study aimed to identify determinants of luminosity threshold, a luminance level at which the surface begins to appear self-luminous. We specifically tested a hypothesis that our visual system knows a maximum luminance level that a surface can reach under the physical constraint that surface cannot reflect more lights that incident lights and apply this prior to determine the luminosity thresholds. Observers were presented a 2-degree circular test field surrounded by numerous overlapping color circles, and luminosity thresholds were measured as a function of (i) the chromaticity of the test field, (ii) the shape of surrounding color distribution and (iii) the color of illuminant lighting surrounding colors. We found that the luminosity thresholds strongly depended on test chromaticity

and peaked around the chromaticity of test illuminants and decreased as the purity of the test chromaticity increased. However, the locus of luminosity thresholds over chromaticities were nearly invariant regardless of the shape of surrounding color distribution and generally well resembled the locus drawn from theoretical upper-limit luminance but also the locus drawn from the upper boundary of real objects. These trends were particularly evident for test illuminants on blue-yellow axis and curiously did not hold under atypical illuminants such as magenta or green. Based on these results, we propose a theory that our visual system empirically internalizes the gamut of surface colors under illuminants typically found in natural environments and a given surface appears self-luminous when its luminance exceeds this heuristic upper-limit luminance.

1. Introduction

Most objects in the real world are visible because they reflect a light. Some objects however themselves emit a light and such self-luminous objects typically have a distinct appearance (e.g. traffic lights visually stand out in a scene). However, any light reaching our retina is indiscriminately encoded by three classes of cone signals regardless of whether the light is reflected from a surface or directly emitted from a light source. Thus, judging whether a given object is self-luminous presents an mathematically underdetermined problem to the visual system. The goal of this study is to reveal how our visual system overcomes this computational challenge and generates the luminous percept.

Self-luminous objects normally have a glowing appearance which is distinct from the appearance of an illuminated surfaces. This qualitative difference was formally

introduced as a mode of color appearance (Katz, 1935). The original description finely discriminates various categories, but this study concerns two modes: surface-color mode and aperture-color mode, which respectively correspond to the qualities of color appearance for an illuminated surface and a self-luminous object. The color appearance was mostly studied in the surface-color mode, and only a limited number of studies investigated the nature of the aperture-color mode (e.g. Uchikawa, Uchikawa & Boynton, 1989).

One common approach is to measure the transition luminance between the surface-color mode and the aperture-color mode which is known as *luminosity threshold.* Past studies investigated what factors might govern the threshold. In early study, Ullman (1976) extensively discussed potential determinants of luminosity thresholds: highest intensity in a scene, absolute intensity of stimulus, local or global contrast, intensity comparison with the average intensity in the scene, and lightness computation. It was concluded that although each factor plays a role, none of these factors are sufficient to predict the luminosity thresholds. Bonato & Gilchrist (1994) reported quantitative observation that an achromatic surface appears luminous when it has roughly 1.7 times luminance of a surface that would be perceived as white. In later years they reported that a surface with a smaller area appears to emit a light at lower luminance level (Bonato & Gilchrist, 1999). For chromatic stimuli, it was repeatedly shown that luminosity thresholds were negatively correlated with stimulus purity in a series of studies (Evans, 1959; Evans & Swenholt, 1967; Evans & Swenholt, 1968; Evans & Swenholt, 1969). They further pointed out the loci of luminosity thresholds over chromaticities are related to the upper-limit luminance of surface colors, known as MacAdam limit (MacAdam 1935a; MacAdam

1935b). Spiegle & Brainard (1996) measured luminosity thresholds using colored real objects placed under illuminants of different color temperatures. They supported Evans' consistent observation about chromaticity-dependent nature of luminosity thresholds and showed that the color of the illuminant also affects luminosity thresholds. They further suggested that the locus of luminosity thresholds can be explained by the physically realizable luminance level with real pigments under an estimated illuminant by a participant. This is an interesting conceptualization linking the luminous percept to illuminant lighting a scene. More recently, Uchikawa et al. (2001) pointed out that the brightness of colored surfaces rather than a physical luminance is highly correlated with luminosity thresholds of colored surfaces. Some studies revealed relation between luminous percept and other perceptual dimensions. For instance, surround stimuli at the same depth as a test field primarily affects the luminosity thresholds (e.g. Yamauchi & Uchikawa, 2005).

These studies well characterized the properties of a test stimulus and of surrounding contexts that have an impact on luminosity thresholds. One implicit assumption here is that visual system bases luminous judgement on external factors available in a scene. Such strategy is prevalent in many other visual judgements. For example, a famous anchoring theory determines a reference based on simple statistics in a given scene (e.g. highest luminance in a scene) which has been successful in explaining empirical results involving lightness judgement (Gilchrist & Bonato, 1995; Gilchrist et al. 1999). Alternatively, visual system might internally hold more absolute criterion for luminous judgement. For instance, it was shown that our visual system might use statistical regularities about possible range of surface color and illuminant color (Judd et al., 1964)

to solve an ill-posed problem such as color constancy (Maloney & Wandell, 1986). Also there are suggestions that color contrast and assimilation arise simply from learning of statistical regularities in external environments (Lotto & Purves, 2000; Long & Purves, 2003). The success of these prior-based approaches implies a possibility that humans might take a similar strategy to make self-luminous judgement.

One primary focus in this study is to reveal whether determinants of luminosity thresholds are externally defined from one scene to another or internally held by visual system regardless of what are present in a scene. We specifically built a hypothesis based on the latter view: visual system internalizes the physical gamut of surface colors under various illuminants and refers to this knowledge when judging whether a given surface is self-luminous. This physical gamut can be visualized by hypothetical surface called optimal colors (MacAdam 1935a, MacAdam 1935b) which will be detailed in General Method section. This hypothesis was specifically led up based on the observation made in a series of color constancy experiments (Uchikawa et al, 2012; Fukuda & Uchikawa 2014; Morimoto et al, 2016; Morimoto et al, 2021). In these studies, we developed a model for illuminant estimation that operated on the assumption that visual system internalizes the gamut of surface colors under various illuminants (i.e. distribution of optimal colors) and the model accounted for observers' estimation of illuminants reasonably well in a variety of conditions. One interpretation of luminosity thresholds is that we visualize the luminance level which visual system assumes as an upper-limit boundary of surface color. Thus, we speculated that loci of luminosity thresholds measured under different illuminants might resemble the locus of optimal colors.

We conducted three experiments to test our hypothesis. In each experiment, we presented a 2-degree circular colored test field surrounded by many overlapping colored circles. We measured luminosity thresholds as a function of test chromaticities. Experiment 1 was designed to test the degree to which luminosity thresholds were influenced by the color statists of surrounding stimuli, in this case the geometry of color distribution. In Experiment 2, we tested the effect of illuminants as well as the shape of surrounding color distribution to reveal whether luminosity thresholds loci agree with optimal color locus under different illuminants (3000K, 6500K and 20000K). In Experiment 3, we measured the loci of luminosity thresholds under atypical illuminants (magenta and green) to investigate whether the loci of luminosity thresholds over chromaticities might differ between chromatically typical and atypical illuminants.

2. General Method

2.1. Computation of physical upper-limit luminance at a given chromaticity

We can compute the theoretical upper-limit luminance at each chromaticity by calculating the chromaticity and the luminance of optimal colors. Here we provide a basic idea of optimal color, but more detailed description is available elsewhere (Uchikawa et al., 2012, Morimoto, 2021). An optimal color is a hypothetical surface having a steep spectral reflectance function as shown in Figures 1 (a) and (b). There are two types (band-pass and band-stop types), and they can have only 0% or 100 % reflectances. Changing λ_1 and λ_2 generate numerous optimal colors ($\lambda_1 < \lambda_2$). To give concrete examples we generated three illuminants of black body radiation (Figure 1 (c)). Then, 102,721 optimal colors were rendered under these illuminants as shown by small dots in Figures 1 (d) and (e). Panel (d) shows L/(L+M) in MacLeod-Boynton (MB) chromaticity diagram

(MacLeod & Boynton, 1979) vs luminance distributions. Panel (e) shows $\log_{10}S/(L+M)$ vs. luminance distributions. To calculate cone excitations, we used the Stockman & Sharpe cone fundamentals (Stockman & Sharpe, 2000).

In the real-world surface reflectance must be less than 1.0 due to a physical constraint, and thus an optimal color has a higher luminance than any other surface that has the same chromaticity. Thus, no real surface can exceed this optimal-color distribution. To show this concretely, we show, in Figures 1(d) and (e), 49,667 objects in the standard object color spectra database for color reproduction evaluation (SOCS, ISO/TR 16066:2003).

From optimal color distributions we see that the physical upper-limit luminance is dependent on the chromaticity. The peak of an optimal color distribution always corresponds to a full-white surface (1.0 reflectance across all wavelengths), which thus corresponds to the chromaticity and intensity of the illuminant itself (so-called white point of the illuminant). For this reason, when the color temperature of illuminant changes, the whole optimal color distribution shift towards the chromaticity of the illuminant without drastically chaning the overall shape. Optimal colors with a higher purity have lower luminance, as they have a narrower-band reflectance and consequently the distribution spreads out as the purity increases. Importantly, once all optimal colors are calculated, we can look for the physical upper-limit luminance at any chromaticity by looking for the luminance of the optimal color at the chromaticity. Interestingly it is notable that the distribution of real objects (SOCS dataset) shows a somewhat similar shape to the optimal color distribution.

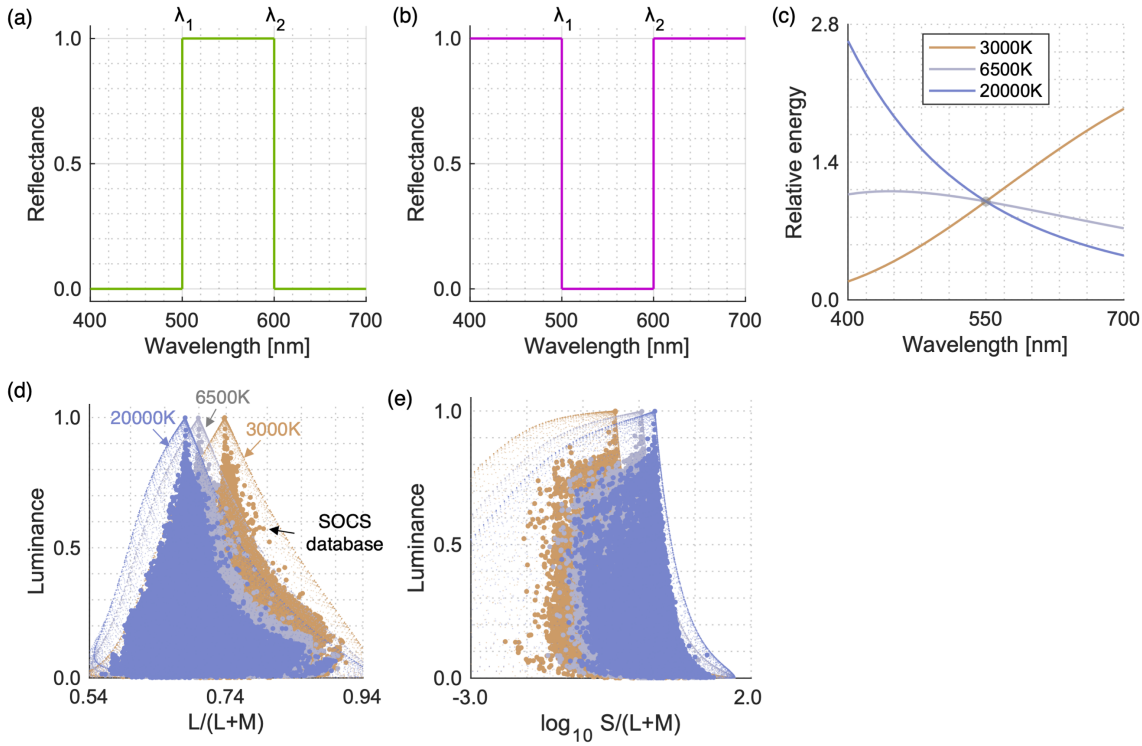

Figure 1: (a), (b) Example optimal colors of band-pass and band-stop types, respectively. (c) Three illuminants defined based on Planck's radiation law. (d), (e) L/(L+M) vs. luminance and $\log_{10}$S/(L+M) vs. luminance distributions, respectively, for optimal colors and SOCS reflectance dataset rendered under 3000K, 6500K and 20000K.

2.2. Estimation of the upper-limit luminance at a given chromaticity for real surfaces

Theoretical upper-limit luminance can be computed through the calculation of optimal color, but the upper-limit luminance for real objects needs to be estimated. Thus, we analyzed 49,672 surface reflectances from SOCS reflectance database (SOCS). This dataset includes reflectances from a wide range of categories of natural and man-made objects: photo (2304 samples), graphic (30,624), printer (7856); paints (229); flowers (148); leaves (92); face (8049); Krinov datasets (370) including natural objects which

were measured in the separate study (Krinov, 1947). We then excluded reflectances that contained a value higher than 1.0 at any wavelength as they might include fluorescent substance. As a result, one reflectance from the printer category and 4 reflectances from the paints category were excluded.

Remaining 49,667 surfaces were then rendered under 6500K, and their chromaticity and luminance were calculated. The luminance value was normalized by that of the full-white surface (100% reflectance at any wavelength). As shown in Figure 2 (a), we plotted chromaticity of all surfaces on the MacLeod-Boynton chromaticity diagram, where L/(L+M) is the horizontal axis and $\log_{10}$ S/(L+M) is the vertical axis. We defined a grid of 25×25 bins and classified 49,667 colors into corresponding bins. Then, for each bin, the maximum luminance across all colors that belong to the bin was defined as the upper-limit luminance of real objects. This procedure was repeated for all 625 bins. The left and center subpanels in panel (b) show the upper-limit luminance for optimal color (for comparison purpose) and real objects. As seen here the locus of the upper-limit luminance for real objects were not smooth. We assumed that this is an artifact due to a limited availability of reflectance samples in the database rather than a nature of reflectances of real objects. Thus, we smoothed the upper-limit luminances based on spatial filtering by 3×3 convolutional filters (each pixel has the value of 1/9). The right subpanel indicates the smoothed data. Note that this upper-limit luminance heatmap is dependent on the color of illuminant. Thus we repeated the same procedure for other black-body illuminants with color temperatures from 3000K to 20000K with 500 K steps. Both optimal color locus and real objects locus unsurprisingly peak at the chromaticity of illuminant shown by the red cross symbol. The upper-limit luminance of real objects

decrease as the stimulus purity increases more sharply than that of optimal colors. We can refer to these look-up-table to find the upper-limit luminance of real objects for an arbitrary chromaticity under illuminant with a range of color temperatures.

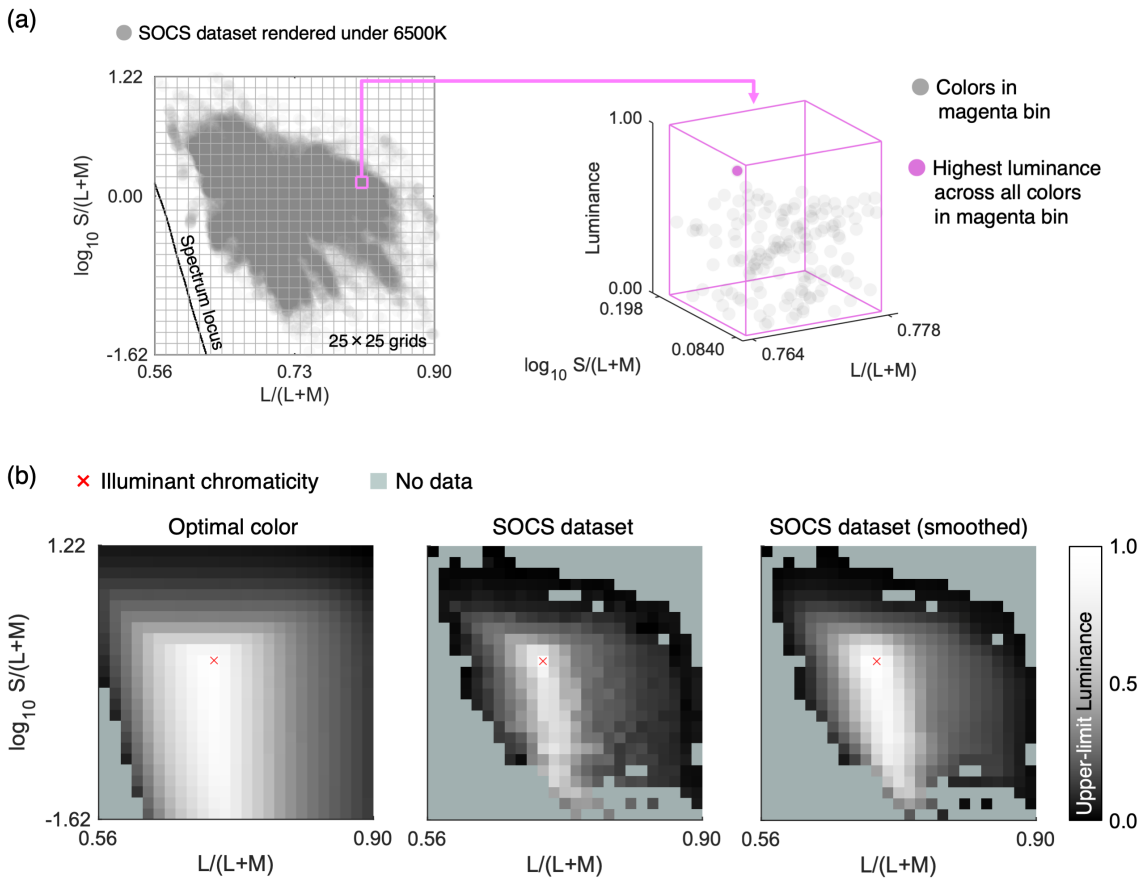

Figure 2: How to estimate the upper-limit luminance for real objects using the SOCS spectral reflectance dataset. 25 × 25 grid was first drawn on MacLeod-Boynton chromaticity diagram. For each grid bin, we searched the surface that has the highest luminance as shown at the right part of panel (a), which was defined as the upper-limit luminance for the chromaticity bin. (b) From left to right, the locus of upper-limit luminance for optimal color, real objects (raw), and real objects (smoothed). The lightness indicates the upper-limit luminance for chromaticity bins. The pale green color indicates there is no data in that bin.

2.3. Observers

Four observers (KK, MI, TM and YK) participated in Experiment 1. KK and YK were also recruited to Experiment 2 as well as two new observers (KS and NT). KK, KS and YK participated in Experiment 3. Observers ages ranged between 22 and 57 (*mean* 31.4, *s.d.* 13.2). Observers were all Japanese. All observers had corrected visual acuity and normal color vision as assessed by Ishihara pseudo-isochromatic plates.

2.4. Stimulus Configuration

The stimulus configuration is shown in Figure 3. The color distribution for surrounding stimuli and chromaticities used for test field are detailed in each experimental section. The spatial pattern was shuffled for each trial.

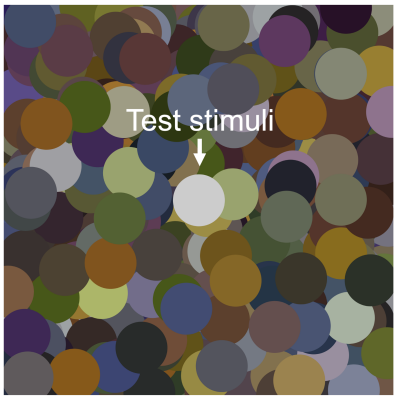

Figure 3: Example of stimulus configuration. The center circle is a test stimulus, and its luminance was adjusted by observers. Each circle had a diameter of 2 degrees in visual angle, and the whole image subtended 15 × 15 degrees. The surrounding color distribution is detailed in each experimental section.

2.5. Apparatus

Data collection was computer-controlled and all experiments were conducted in a dark room. Stimuli were presented on a cathode ray tube (CRT) monitor (BARCO, Reference Calibrator V, 21 inches, 1844 × 1300 pixels, frame rate 95Hz) controlled with ViSaGe (Cambridge Research Systems), which allows 14-bit intensity resolution for each of RGB phosphors. We conducted gamma correction using a ColorCAL (Cambridge Research Systems) and spectral calibration was performed with a PR650 SpecrtaScan Colorimeter (Photo Research inc.). Observers were positioned 114 cm from the CRT monitor and the viewing distance was maintained with a chin rest. Observers were asked to view the stimuli binocularly.

2.6. General procedure

Observers first dark-adapted for 2 mins and then adapted to an adaptation field for 30 seconds. The adaptation field was the full uniform screen that had either the chromaticity of 6500K (Experiments 1 and 3) or the chromaticity of test illuminant (Experiment 2), and in either case the luminance was equal to mean luminance value across surrounding stimuli. Then, the first trial began. We drew surrounding stimulus circles so that they had a specific color distribution as detailed in each experimental section. The 2-degree circular test field was presented at the center of the screen. The test field was never occluded by surrounding stimuli. Observer's task was to adjust the luminance of the test field to the level at which the surface-color mode changed to the aperture-color mode. The ambiguity regarding the criterion to judge the transition between surface-color mode and aperture-color mode was reported in a past study (Speigle & Brainard, 1978, Uchikawa et al., 2001). This is mainly because the transition is not sharp, and there is a

range that a surface can appear the mixture of surface-color mode and aperture color mode. We took care this issue and instructed observers to set the luminance value to the halfway between the upper-limit of the surface color mode and the lower-limit of the aperture color mode. During the experiments, observers were instructed to view whole stimuli rather than fixating at a specific point to avoid local retinal adaptation. The initial luminance value for the test field was randomly chosen from 2.0, 5.0, 8.0, 11.0, 14.0, 17.0, 20.0, 23.0, 26.0 and 29.0 cd/m^2. Specific experimental conditions are detailed in each experimental section.

3. Experiment 1

3.1 Surrounding color distribution, test illuminant and test chromaticity

In a natural scene, the colors of objects tend to cluster around the white point of illuminant and the density of colors decreases as purity increases. Consequently, the color distribution tends to form a mountain-like shape as shown in Figure 1 (d). The aim of Experiment 1 was to investigate how loci of luminosity thresholds change when thresholds are measured in a scene that has an atypical shape of color distribution. In an extreme case, where observers purely rely on internal criteria to judge self-luminous surface, the luminosity thresholds should not change at all regardless of surrounding color distribution. However, in contrast if observers make a self-luminous judgement using surrounding colors, for example by estimating the upper luminance boundary from surrounding distribution, luminosity thresholds should largely change depending on the shape of surrounding color distribution.

Figure 4 (a) shows the five surrounding color distributions used in Experiment 1. The

6500K illuminant on the black-body locus was chosen as a test illuminant in this experiment. We first defined *natural* color distribution at upper-left subpanel and then transformed the distribution to generate 4 atypical color distributions (*reverse*, *flat*, *slope+* and *slope-*) in following ways. First, to construct the *natural* color distribution, we used dataset of 574 spectral reflectances of natural objects (Brown, 2003). Out of 574 reflectances, 516 reflectances were inside the chromaticity gamut of the experimental CRT monitor when rendered under the 6500K test illuminant. All stimuli were presented via a ViSaGe, which had the technical constraint that only 253 colors can be simultaneously presented. Thus, we selected 253 reflectances samples out of 516 reflectances so that when rendered under 6500K, 253 colors approximately spatially uniformly distribute in a three-dimensional color space (L/(L+M), S/(L+M) and L+M).

To generate the other color distributions (*reverse*, *flat*, *slope+* and *slope-*), we independently scaled each of 253 reflectances by a scalar value to manipulate the luminance while keeping the chromaticity constant. The inserted image in each subpanel shows an example of surrounding stimuli that has a corresponding color distribution. Note that the spatial layout of surrounding stimuli was shuffled for each trial. For all distributions, the intensity of test illuminant was determined so that a full-white surface (i.e. 100% reflectance across all visible wavelengths) had the luminance of 35.0 cd/m^2 under the test illuminant.

For the center test field, we chose 9 reflectances from the 253 reflectances so that they fall closely on the black-body locus when placed under 6500K illuminant. The panel (b) in Figure 4 shows these 9 test chromaticities at which luminosity thresholds were

measured.

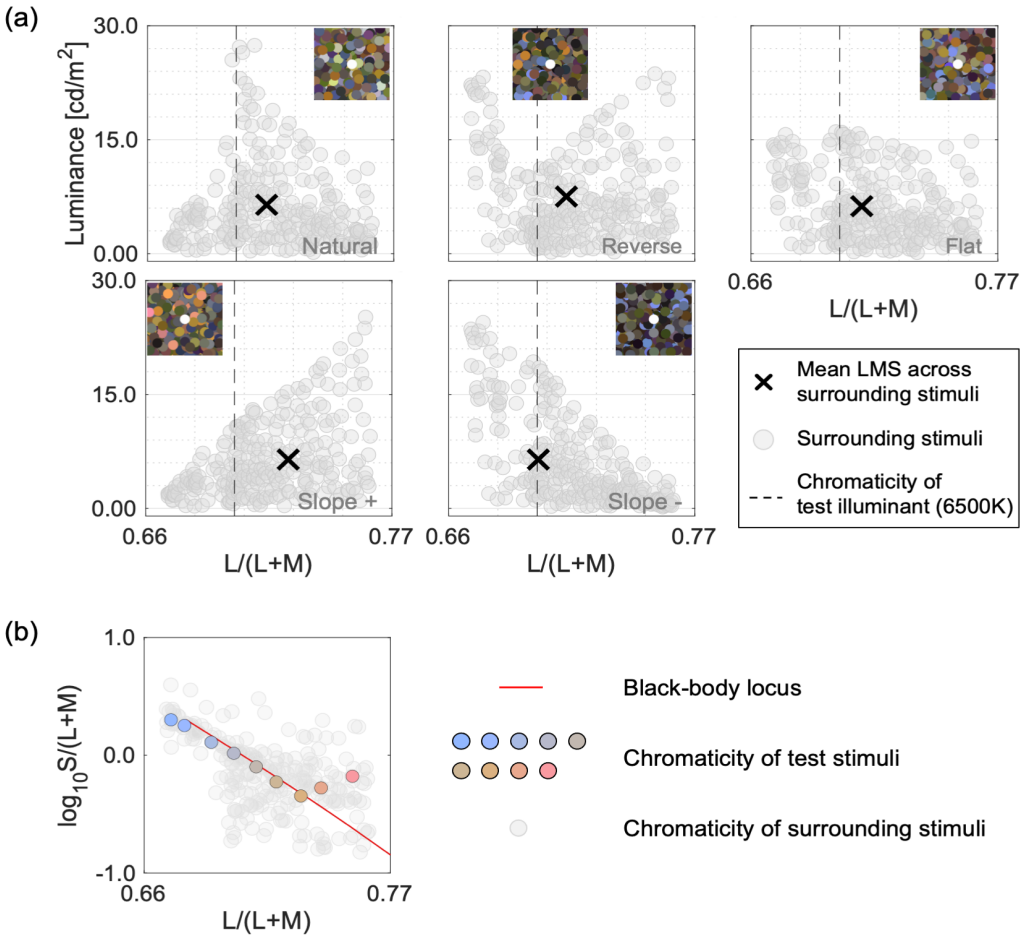

Figure 4: (a) 5 color distribution sets for surrounding stimuli. An inserted image at top part shows an example stimulus configuration for each color distribution. The vertical dashed black line indicates L/(L+M) value of 6500K test illuminant. Black cross symbols indicate mean cone response across all 253 surrounding stimuli. (b) 9 test chromaticities at which the luminosity thresholds were measured.

3.3 Procedure

One block consisted of 9 settings to measure thresholds at all 9 test chromaticities in a random order. There were 5 blocks in each session to test all 5 distribution shapes. The

order of distribution condition was randomized. All observers completed 20 sessions in total (i.e. 20 repetitions for each data point). They completed 10 sessions per day and thus experiments were conducted in two days.

3.3 Results

Figure 5 shows results in Experiment 1. Colored symbols with error bars indicate each observer's setting. Each data point is the average across 20 repetitions. The average across 4 observers is shown by black circles. There were some variations across individuals. Furthermore, the experimental design was to try to collect reliable data from a small number of participants. Thus, we argue results individually. The magenta circles show luminances of optimal colors at test chromaticities when rendered under the test 6500K illuminant (the optimal color locus). In other words, if the visual system uses the optimal color to judge whether a surface emits a light, the observers setting should match the magenta line. The blue line shows a smoothed upper-limit luminance locus of real objects, estimated from SOCS reflectance dataset as shown in Figure 2, which more rapidly decreases as it gets away from the white point than the optimal color locus does. For simplicity, we hereafter refer to the magenta and blue lines as predictions of the optimal color model and the real object model, respectively.

First, all observers showed that loci of luminosity thresholds show the mountain-like shape regardless of surrounding color distribution. The loci generally peaked around the chromaticity of a test illuminant (the vertical black dashed line) and the luminosity threshold decreases as the test chromaticity gets away from the white point. Although there are some individual differences, especially in the overall setting level (e.g. KK

generally has higher thresholds than others) and in the peak chromaticity, the luminosity thresholds generally seem to be more resemble the prediction of the optimal color model than that of the real object model in this experiment. This is consistent with the hypothesis that the visual system knows the upper boundary of the optimal color distribution and judges that a given surface is self-luminous when its luminance exceeds the luminance of optimal colors.

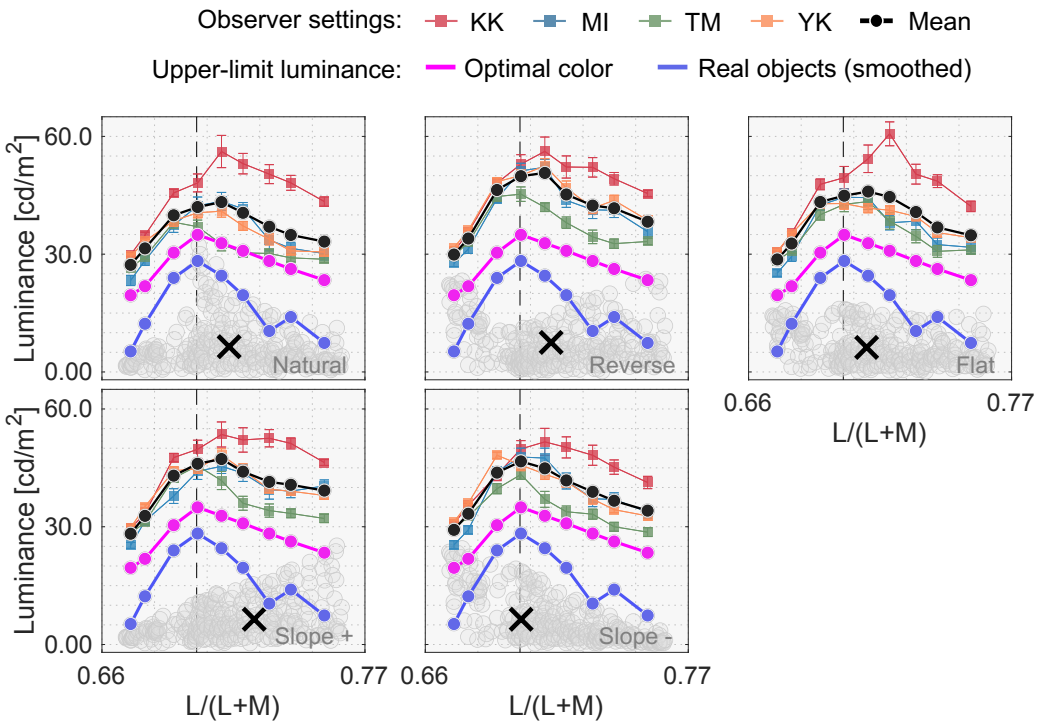

Figure 5: Colored square symbols indicate averaged settings across 20 repetitions for each observer. The error bar indicates ± S.E across 20 repetitions. The black circle symbols indicate average observer settings (n = 4). The magenta circle symbols denote the luminance of the optimal color at test chromaticities and thus indicate the physical upper-limit luminance. The blue line shows the upper-limit luminance of real objects estimated from the SOCS reflectance dataset. The vertical dashed line shows the chromaticity of the test illuminant (6500K). The black cross symbol indicates mean LMS value across surrounding stimuli.

To quantify the similarity between observers and models, we calculated Pearson's correlation coefficient between observer settings and model predictions over 9 test chromaticities. The Figure 6 shows summary matrices of correlation coefficient. We calculated correlation coefficients for each observer and discuss them on an individual basis.

The magenta and blue symbols indicate the optimal color model and the real object model, respectively. In addition, we evaluated a model to judge the self-luminous surface when its luminance exceeds the surrounding color distribution. The luminosity thresholds estimated from such model should show the similarity to the shape of surrounding color distribution. For example, in the reverse condition, the luminosity threshold should be lowest at white point and increase as the saturation of the test stimulus increases. This model is labelled as "surrounding color" in the Figure 6. Note that this is a simplified model, and it is unlikely that visual system takes such strategy. Instead, our goal here was to build a framework in which we quantitatively predict an observer's behaviour if she/he judges the luminosity thresholds solely based on what's externally presented in each trial without using any prior about statistics in the real world.

The cyan star symbols in some cells indicate the highest correlation-coefficient value across 3 tested models. The cyan arrows below each subpanel indicates the model that received the highest number of cyan stars across 4 observers.

Overall, since the observer settings are stable across all distribution conditions, the correlation coefficient patterns are also similar between the optimal color and the real object models whose prediction are both not affected by surrounding colors. However, the correlation coefficients for the surrounding color model strongly depend on distribution condition as predicted. Specific trends are as follows. For observers KK and MI, the loci of luminosity thresholds showed highest correlation with the optimal color model for all distributions. For TM, the real object model was the best predictor in all distributions except for the Flat condition. For YK, the optimal color model showed the highest correlation for *reverse*, *flat* and *slope+* conditions while the real object model showed the highest correlation for *natural* and *slope-* conditions. If we summaries these trends based on the number of cyan arrows each model received, the optimal color model is the best predictor in Experiment 1.

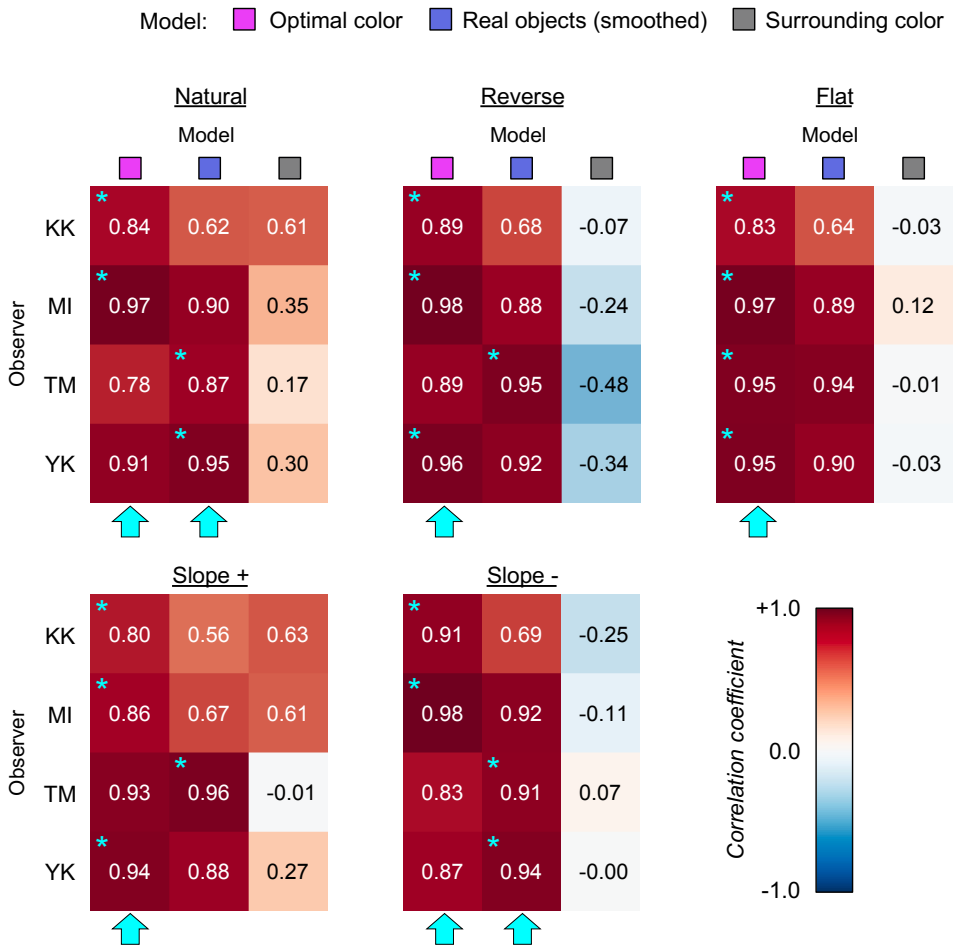

Figure 6: The matrices of Pearson's correlation coefficient calculated between observer settings and model predictions over 9 test chromaticities. Each subpanel indicates each distribution condition (*natural*, *reverse*, *flat*, *slope+* and *slope-*). The color of individual cell indicates the correlation coefficient as denoted by the color bar. The cyan star symbol indicates the highest correlation coefficient across 3 models. The cyan arrows at the bottom of each subpanel show the model that received the highest number of cyan star marks, indicating a good candidate model of human observers' strategy to judge the self-luminous surface.

The major finding in this experiment is that the loci of luminosity thresholds are nearly

invariant regardless of the shape of surrounding color distribution. This result supports the idea that observers use an optimal color distribution as an internal reference to determine the luminosity thresholds rather than what is presented in a scene. In Experiment 2, we tested whether this observation holds under different illuminants which changes the shape of optimal color distribution as shown in Figure 1. If the visual system indeed uses the optimal color, the luminosity thresholds should also follow the change in a consistent way that optimal color distribution changes.

4. Experiment 2

4.1 Surrounding color distribution, test illuminant and test chromaticity

We employed *natural*, *reverse* and *flat* distributions of surrounding colors. For test illuminants, we used 3000K, 6500K and 20000K on the black-body locus whose spectral distributions are shown in panel (c) of Figure 1. For surrounding stimuli, we sampled 180 out of 253 reflectances used in Experiment 1 that were inside the chromaticity gamut of the experimental CRT monitor under all test illuminants. The panel (a) in Figure 7 shows all 9 test surrounding conditions (3 distributions × 3 test illuminants).

We then selected 15 surface reflectances from the 180 reflectances. The panel (b) shows the 15 test chromaticities when rendered under each test illuminant at which the luminosity threshold was measured.

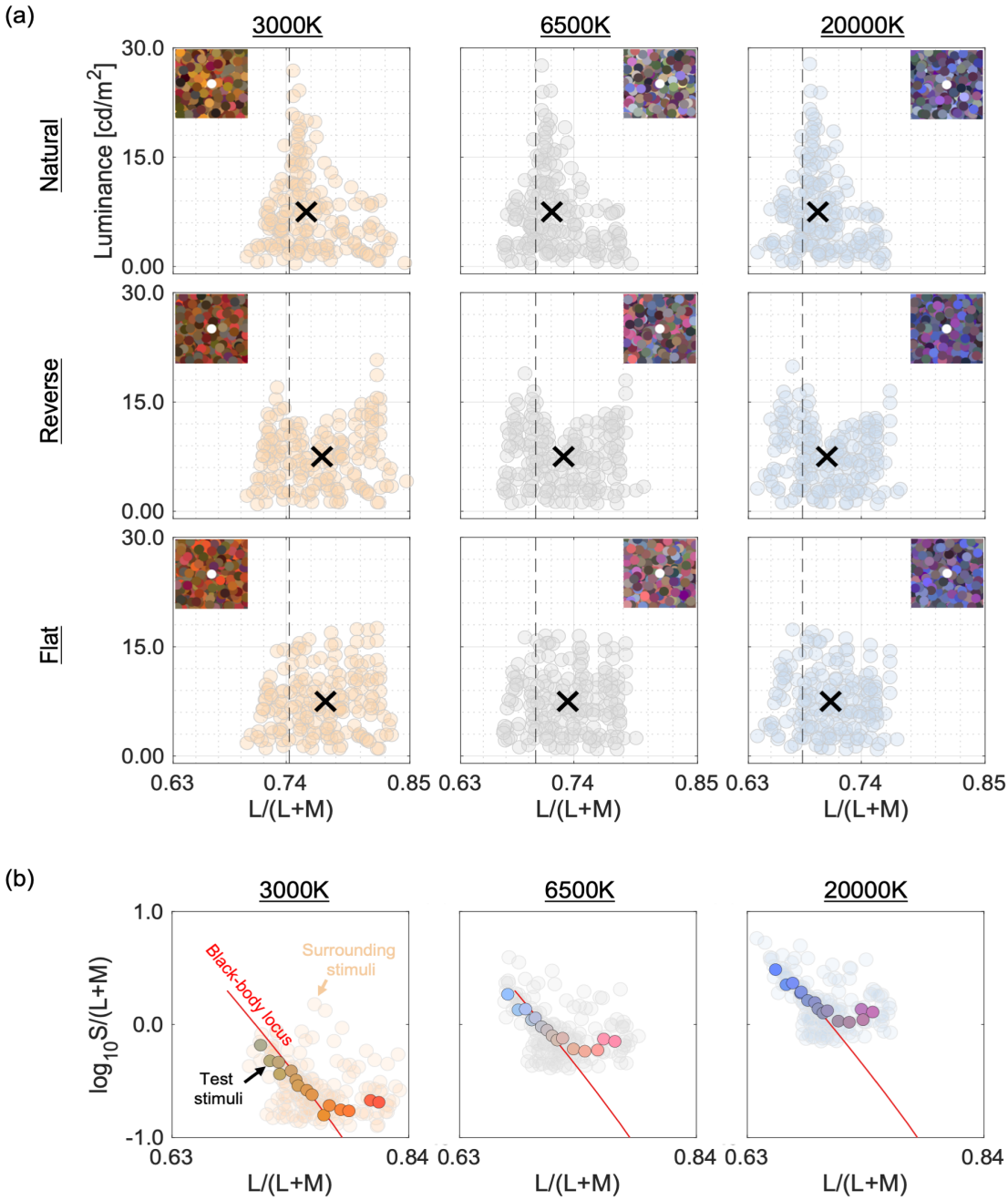

Figure 7: (a) 9 color distributions for surrounding stimuli (3 test illuminants × 3 distributions). Inserted image shows an example stimulus configuration. The vertical dashed black line indicates the L/(L+M) value of each test illuminant. Black cross symbols indicate mean cone response values across 180 surrounding stimuli. (b) 15 test chromaticities at which the luminosity threshold was measured.

4.2 Procedure

One block consisted of 15 consecutive settings to measure thresholds for all test chromaticities presented in a random order. There were 9 blocks in one session to test all conditions (3 illuminants × 3 distributions). The order of condition was randomized. All observers completed 10 sessions in total. The experiment was conducted in three days.

4.3 Results

The black line in Figure 8 shows the mean setting across 4 observers. The rest of the data presentation follows the result in Experiment 1. For the clarity, only the averaged setting is shown here, but the individual observers' data is presented in Figure S1 in Supplementary material.

First, the mean settings showed that the locus of luminosity thresholds were again mountain-like shape, and the influence of the shape of surrounding color distribution was almost absent, supporting the finding in Experiment 1. It is also noticeable that the peak chromaticity of the mean setting in each panel shifted towards the illuminant chromaticity shown by vertical dashed lines.

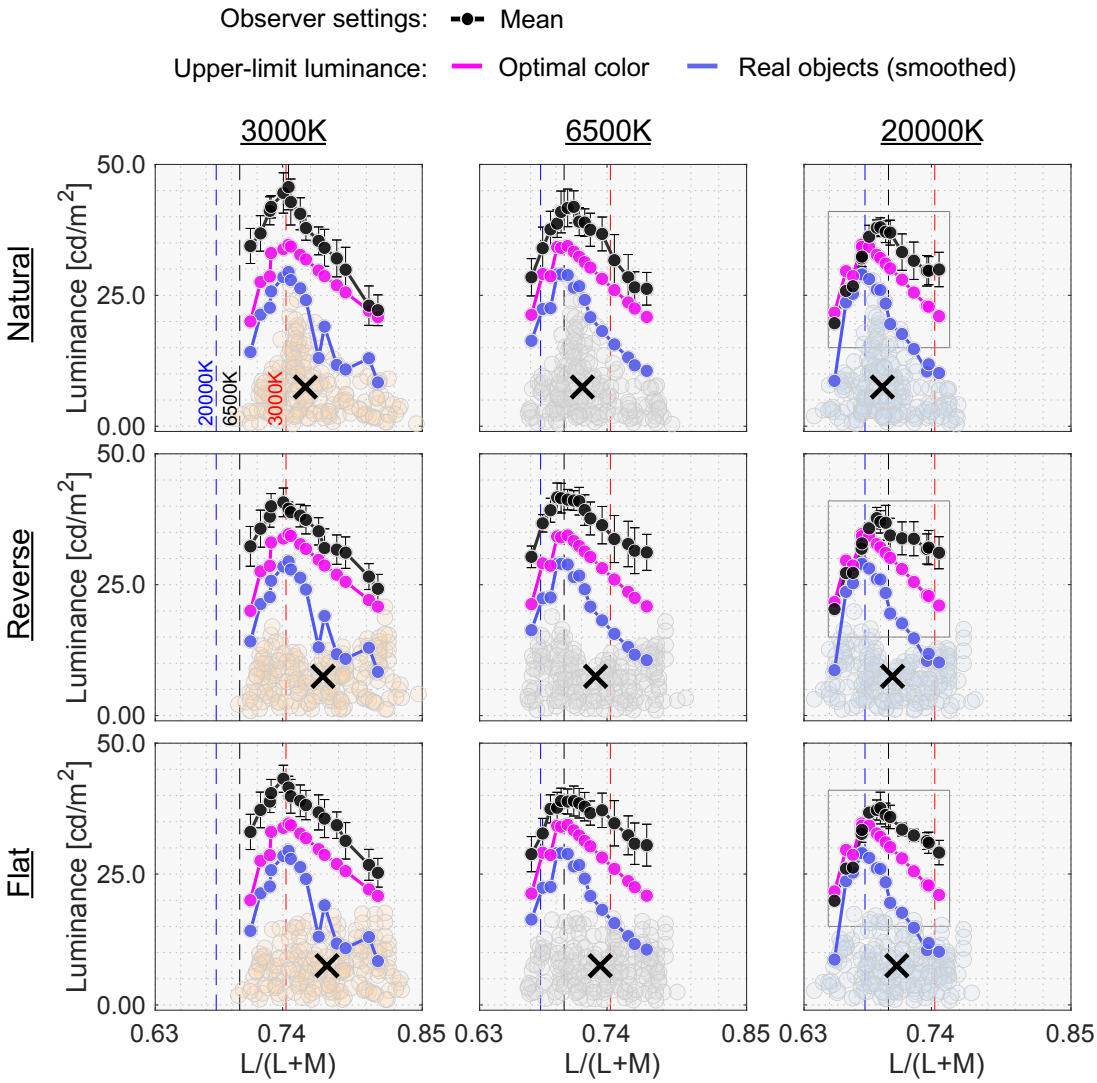

Figure 8: The black circle symbols indicate average observer settings (n = 4). The error bar indicates ± S.E across 4 observers. The magenta circle symbols denote the optimal color locus. The blue line shows the upper-limit luminance of real objects. The red, black and blue vertical dashed lines show the chromaticities of test illuminants of 3000K, 6500K and 20000K, respectively. The black cross symbol indicates mean LMS value across surrounding stimuli. The individual observer data is shown in supplementary material. A region surround by a rectangle in 20000K condition are further discussed in Figure 9.

It should be noted that the peak chromaticity of luminosity threshold loci for 20000K was slightly shifted to higher L/(L+M) direction from the chromaticity of the test illuminant. This trend was generally consistent across observers as shown in Figure S1. One potential reason would be that observers misestimated the illuminant color from the surrounding colors. Human color constancy is often imperfect, and thus we speculated that observers' luminance settings might better agree with the optimal color or real objects rendered under an illuminant estimated by each observer instead of a ground-truth illuminant (20000K). In fact allowing misestimate of illuminant color was also reported be an important factor in predicting luminosity thresholds by Spiegle and Brainard (1990). The estimated illuminant is normally measured using a technique such as achromatic setting (Brainard, 1998), but these data were not collected in this study. Thus, we assumed the peak chromaticity of observer settings as the observer's estimated illuminant.

We first calculated the chromaticities of illuminants from 3000K to 20000K in 500K steps. Then, for each observer and for each condition independently, we searched the color temperature that has the closest chromaticity to the peak chromaticity of the luminosity thresholds. Table 1 summarizes color temperatures of the estimated illuminants in each condition. In 3000K condition, estimated illuminants matched ground-truth color temperature for most observers. For 6500K, there was a slight variation across observers. It is notable that in 20000K condition that observers estimated color temperatures substantially lower than those of the ground-truth.

Table1: Estimated illuminant by each observer judged from the chromaticity at which luminosity thresholds peaked. The top row shows the color temperatures of ground-truth illuminants and the numbers in other cells indicate the color temperature of estimated illuminants.

		3000K	6500K	20000K
Natural	KK	3000	5500	10500
	KS	3000	7000	8500
	NT	3000	5000	10500
	YK	3000	5500	12000
Reverse	KK	3000	6500	7500
	KS	4000	7000	7500
	NT	3000	5500	12000
	YK	3500	5000	10500
Flat	KK	3000	7000	8500
	KS	3000	5000	8500
	NT	3000	5500	12000
	YK	3000	6500	12000

Then, we drew optimal color loci under these estimated color temperatures. This concept is depicted in Figure 9. Intuitively speaking this procedure allows us to equate the peak between the optimal color locus and the measured luminosity thresholds locus. The pale magenta curve shows the optimal colors under the estimated illuminant and seems to predict mean observer settings better than the optimal color locus under the ground-truth illuminant (20000K).

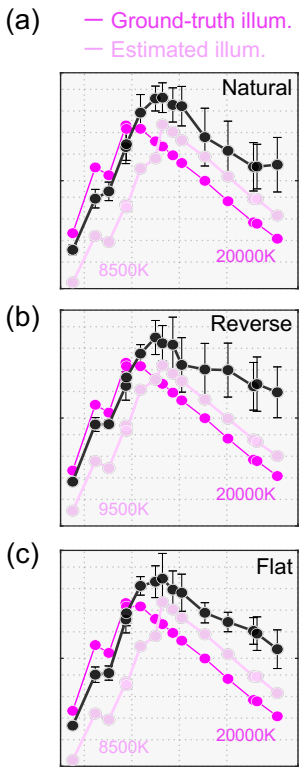

Figure 9: Optimal color models based on ground-truth illuminant (magenta) and based on estimated illuminants for averaged observer setting (pale magenta). It is shown that observers' settings are better explained by the optimal color model that allows misestimation of illuminants by observers.

Figure 10 indicates correlation coefficient matrices for all conditions. We compare correlations from 5 models: (i) optimal color model and (ii) real object model under ground-truth illuminant, (iii) optimal color model and (iv) real object model under estimated illuminant, and (v) surrounding color model. Again, the cyan star symbol in cells indicates the highest correlation across 5 models for that participant. The cyan arrows below each subpanel indicates the model that has the highest number of cyan stars indicating the overall best model for that condition.

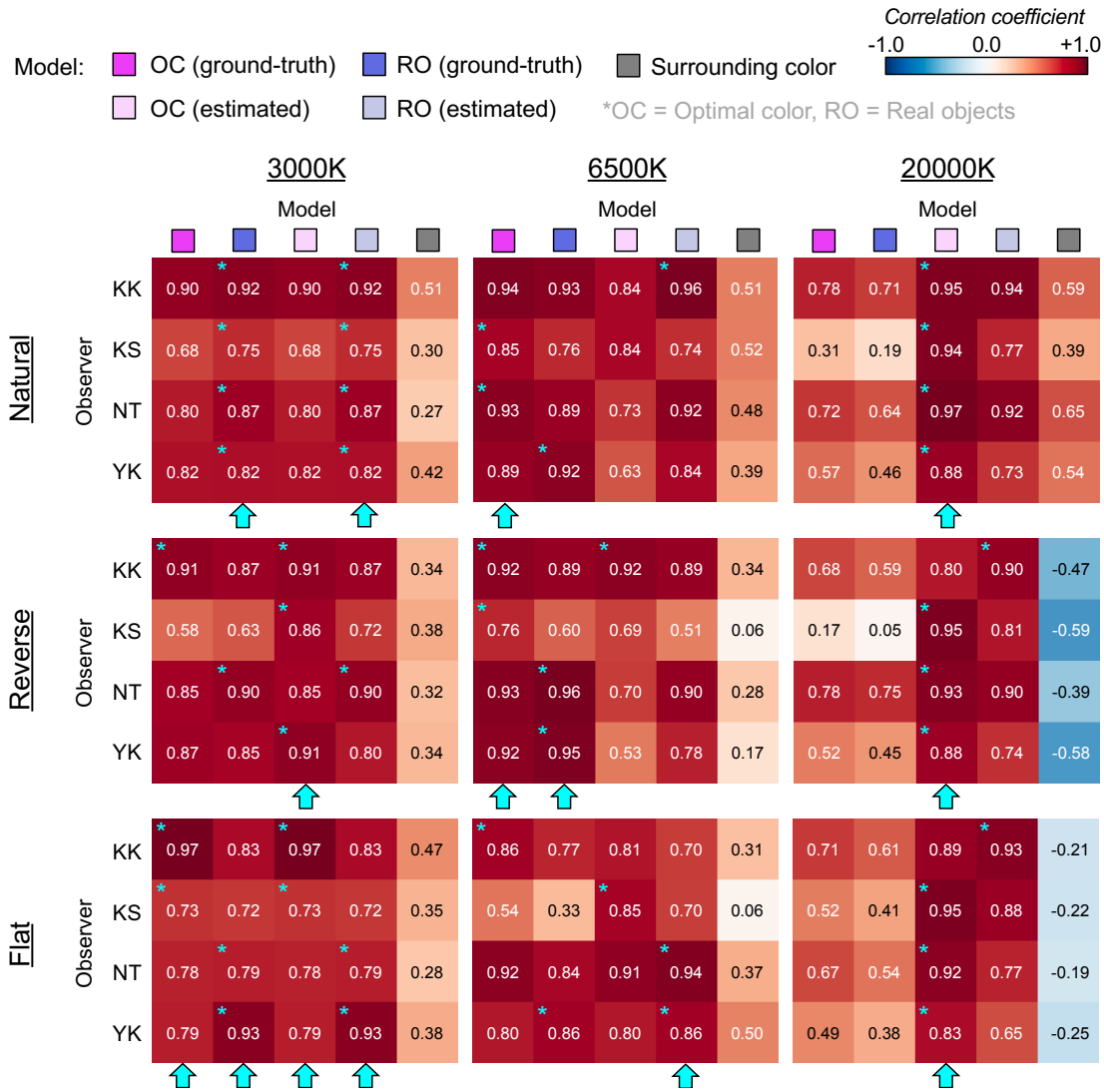

Figure 10: The matrices of Pearson's correlation coefficient calculated between observer settings and model prediction over 15 test chromaticities. The cyan star symbol indicates the highest correlation coefficient across 5 models. The cyan arrows at the bottom of each subpanel show the model that received the highest number of cyan star mark.

Overall, the surrounding color model does not show high correlation with observer settings in any condition, agreeing with the trends in Experiment 1. The optimal color

model and the real object model seem to show high correlation, and it depends on the condition whether which model shows a higher correlation. For 3000K, *natural* condition shows highest correlation was found for the real object model, consistently across all observers. For *reverse* condition, all observers except NT showed highest correlations with the optimal color model under estimated illuminant while for *flat* condition the votes were split between optimal color and real object models. For *natural*-6500K, KS and NT were well predicted by the optimal color model under ground-truth illuminant, but other two observers were better correlated with the real objects model. For *reverse* condition, the optimal color and the real object model both show high correlation. The real object model under estimated illuminant predicted best in *flat* distribution condition. It is notable that for 20000K condition, the optimal color model under the estimated illuminant was consistently the best predictor. It is also shown that the optimal color model under the ground-truth illuminant shows much lower correlations, suggesting that considering observers' misestimate of illuminants plays a role in predicting luminosity thresholds. In summary both the optimal color model and the real object model both showed a fairly good agreement with human observers' settings.

Experiments 1 and 2 collectively suggested that both optimal color locus and real object locus seemed to be a good candidate determinant of luminosity thresholds. One noteworthy feature in Experiments 1 and 2 is that we used illuminants on blue-yellow axis that are typically found in natural environments. We also used chromaticities on black-body locus for the test field. If we assume that visual system learns the locus of optimal color distribution or real objects distribution through observing colors in natural

environments, luminosity thresholds under atypical illuminants may not well agree with prediction of the optimal color model or the real object model. We directly tested this hypothesis in Experiment 3.

5. Experiment 3

Experiment 3 tested whether luminosity thresholds resembled optimal color locus under atypical illuminants. We also chose a wider range of test chromaticities from the black-body locus and a locus that is orthogonal to the black-body locus.

5.1 Surrounding color distribution, test illuminant and test chromaticity

We employed *natural*, *reverse* and *flat* for surrounding distributions. For test illuminants, we used magenta and green illuminants. We chose two color filters (Rosco, R44 “Middle Rose” and R4460 “Calcolor 60 Green”) and 6500K illuminant was passed through these filters to obtain the spectra shown Figure 11 (a). The chromaticities of these illuminants largely deviate from black-body locus as shown in panel (b). Out of the 574 spectral reflectances of natural objects collected by Brown, 251 reflectance were inside the chromaticity gamut of the CRT monitor under both illuminants. For surrounding stimuli, we sampled 180 reflectances out of the 251 reflectances and created each distribution following the manipulation used in Experiments 1 and 2.

Panel (a) in Figure 12 shows surrounding distributions for all 6 test conditions (3 distributions × 2 test illuminants). The intensities of test illuminants were determined so that average luminance across 180 colors matches 2.5 cd/m^2.

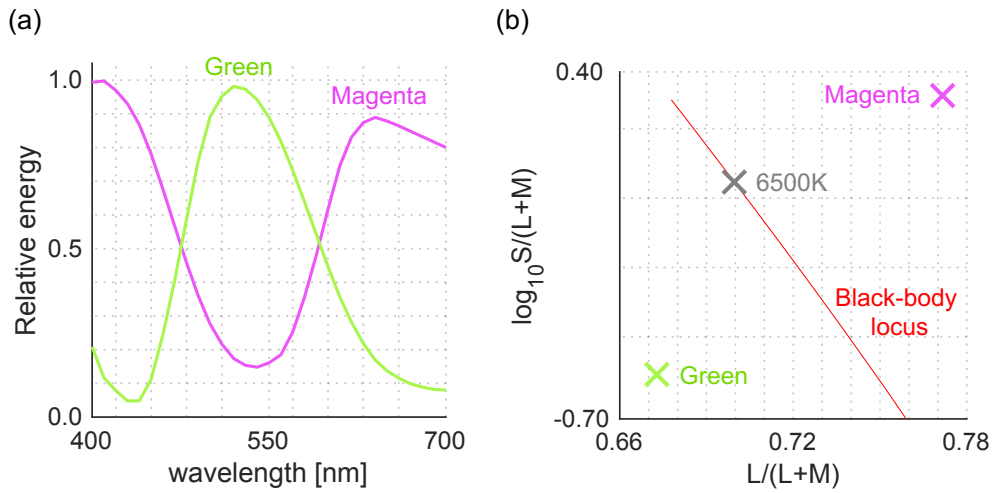

Figure 11: (a) Spectra for magenta and green illuminants used in Experiment 3. (b) Chromaticities of both illuminants. The black-body locus and the chromaticity of 6500K illuminant are shown for the comparison purpose.

For the test field, 8 reflectances were selected from the 180 reflectances and they were used under both illuminant conditions. Then, we sampled different 5 reflectances separately for each illuminant condition. The panel (b) shows 13 chromaticities when rendered under each test illuminant. The 5 data points surrounded by a red edge indicates the 5 reflectances that were not shared between illuminant conditions. In this experiment, the test chromaticities were chosen so that their chromaticities vary along two directions: (i) the black-body locus (shown by circles symbols) and (ii) an axis approximately orthogonal to the black-body locus (shown by triangle symbols). There were 7 chromaticities for each direction, but there was one chromaticity used for both directions (shown by the black square symbol). The chromaticities of natural objects tend to spread along black-body locus, and the purpose of this design was to test whether luminosity thresholds measured at atypical chromaticities would deviate from the prediction of optimal color model or real object model.

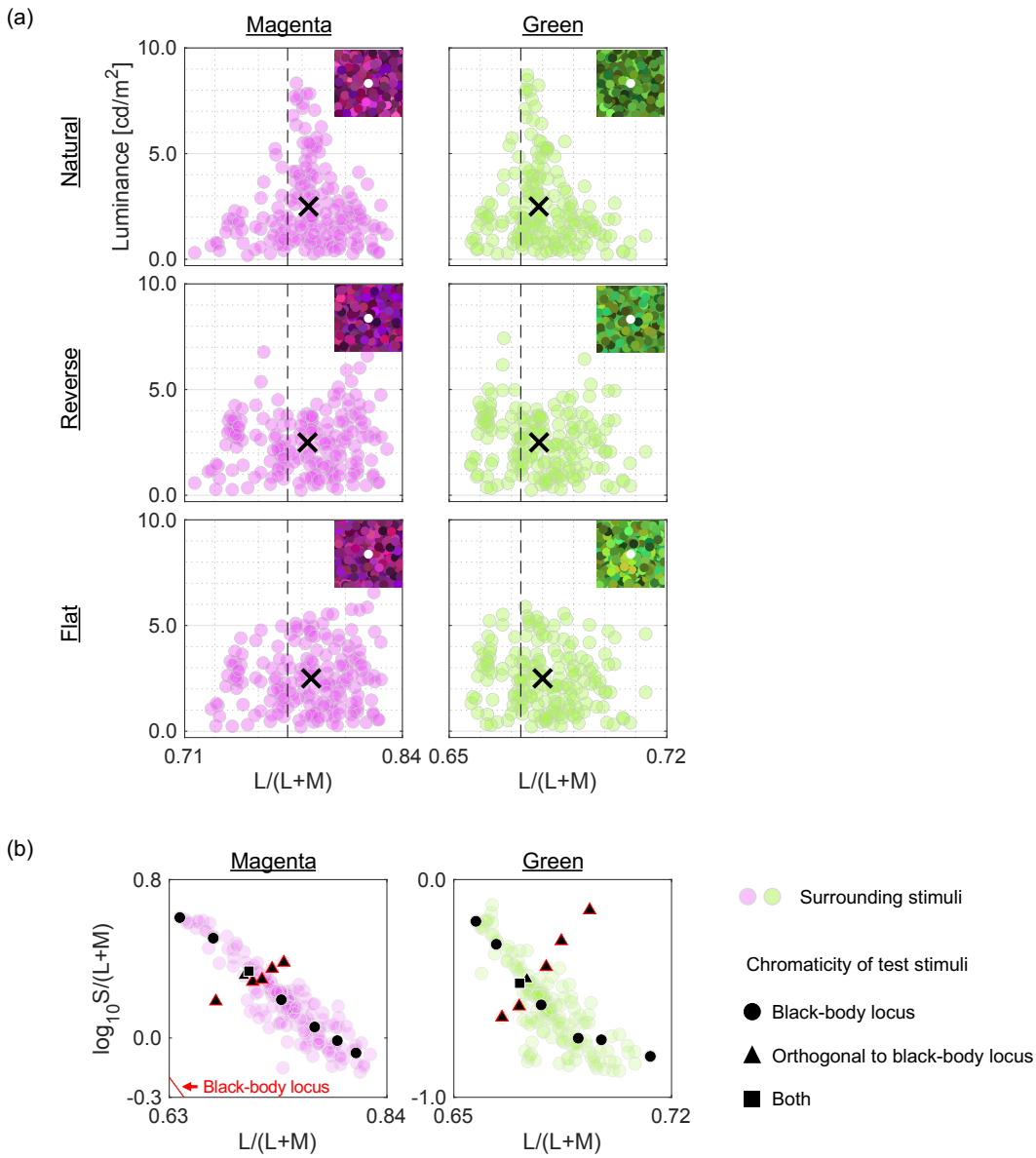

Figure 12: (a) 6 color distributions for surrounding stimuli (2 test illuminants × 3 distributions). Inserted image shows an example stimulus configuration. The vertical dashed black line indicates the L/(L+M) value of test illuminant. Black cross symbols indicate mean cone response values across 180 surrounding stimuli. (b) 13 test chromaticities at which the luminosity threshold was measured. Symbols with a red edge indicates reflectances that were not shared between magenta and green illuminants.

5.2 Procedure

One block consisted of 13 consecutive settings and thresholds were measured for all test chromaticities in a random order. Each session comprised 6 blocks to test all distribution × illuminant conditions. The order of condition was randomized. All observers completed 10 sessions in total. Experiments were conducted in two days, and observers completed 5 sessions per day.

5.3 Results

Figure 13 shows results. Left 6 panels show luminosity thresholds measured at chromaticities on black-body locus (black circles and the square in panel (b), Figure 12) while right 6 panels indicate thresholds at chromaticities on the orthogonal locus (black triangles and the square in panel (b), Figure 12).

We first look at left two columns. For magenta illuminant condition, observers' settings again show a mountain-like shape. Also, it is shown that settings are not dependent on surrounding color distribution. However, in this condition optimal color model and real object model show relatively flat locus. For green illuminant, observer settings appear flat. Also luminosity thresholds for subject KS show a fairly different trends from the other observers, and the locus is not well predicted by optimal color locus nor real object locus, which was not observed in Experiments 1 and 2.

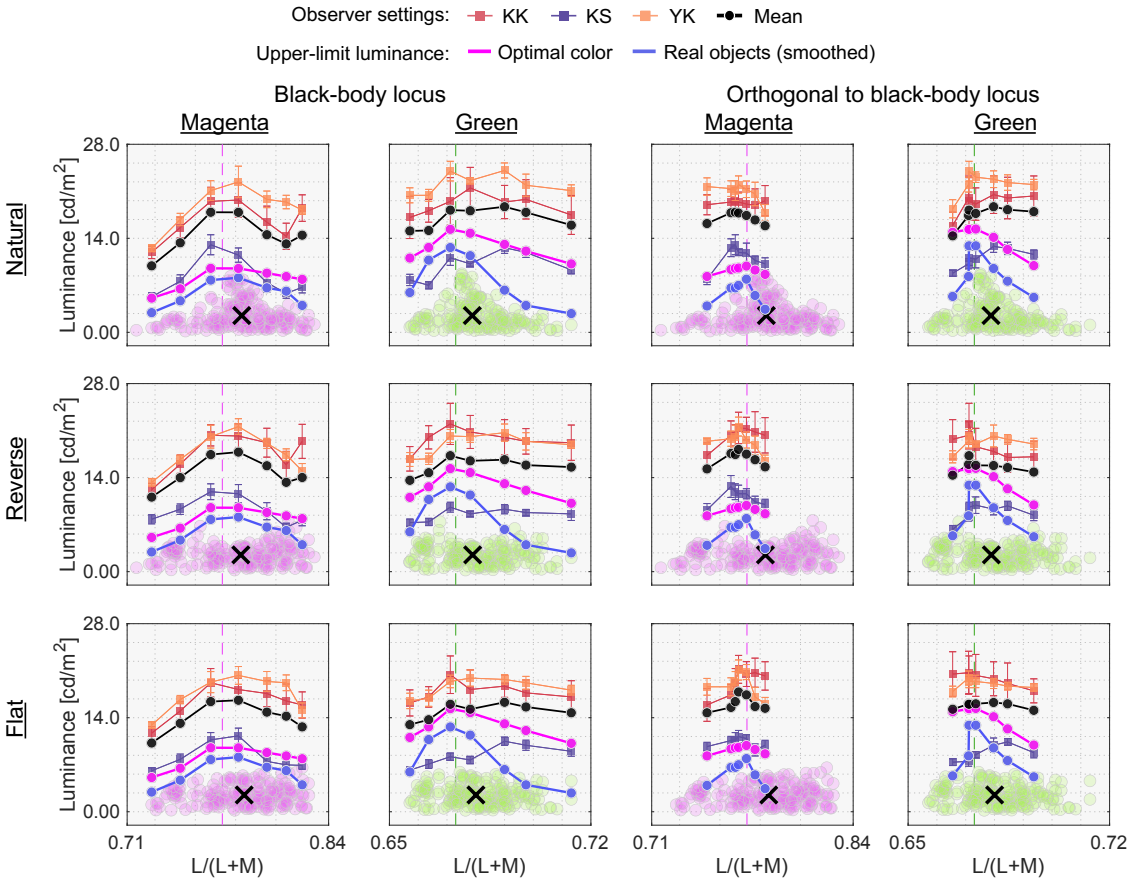

Figure 13: Observer settings in in Experiment 3. Left two columns indicates luminosity thresholds measured at test chromaticities on black-body locus (circle and square symbols in panel (b), Figure 12). Right two columns show test chromaticities on the locus orthogonal to black-body locus (triangle and square symbols in panel (b), Figure 12). Colored square symbols indicate averaged setting across 10 repetitions for each observer. The error bar indicates ± S.E across 10 repetitions. The black circle symbols indicate average observer settings (n = 3). The magenta circle symbols denote the optimal color locus and the blue line shows the real objects locus. The vertical dashed line shows the chromaticity of the test illuminant. The black cross symbol indicates mean LMS value across surrounding stimuli.

When the test chromaticities are on the axis orthogonal to the black-body locus (right two columns), for magenta condition all observers' settings might appear to resemble the optimal color locus at a first glance. However for green illuminant condition, KS again shows different trend from other observers and all observers do not agree with the prediction of the optimal color model nor the real object model.

Figure 14 allows us to compare the correlation coefficient across models and conditions. For the leftmost column, the optimal color model showed overall good correlation for *natural* condition, while the real object model showed good correlation for *reverse* and *flat* conditions. For *natural* condition, KS shows highest correlation with surrounding color model, which was not observed in Experiments 1 and 2 in which illuminants on black-body locus were used as test illuminants. For the second leftmost column, in most cells correlation coefficients appear considerably low. Although the optimal color model consistently showed highest correlation for all distribution conditions (average coefficient across 9 cells is 0.58), the correlation coefficient is not so high if we consider that the correlation for the optimal color model was 0.901 in Experiment 1 (average across 5 distributions × 4 observers). Also, in Experiment 2, correlations were 0.746 for the optimal color model of ground-truth illuminant and 0.837 for estimated illuminant (average across 9 conditions × 4 observers in both cases).

For right two columns, for magenta illuminant condition, the trend seems to be close to that of test chromaticities on black-body locus (leftmost column), but correlation coefficient overall seems to be lower. For green-natural condition, the closest color shows a high correlation with observers KK and KS. It is notable that the optimal color

model shows nearly zero or even negative correlations. For reverse condition, real objects showed the best correlation, but their values are not high (0.577, average across 3 observers). For flat condition, we did not find a consistently good model.

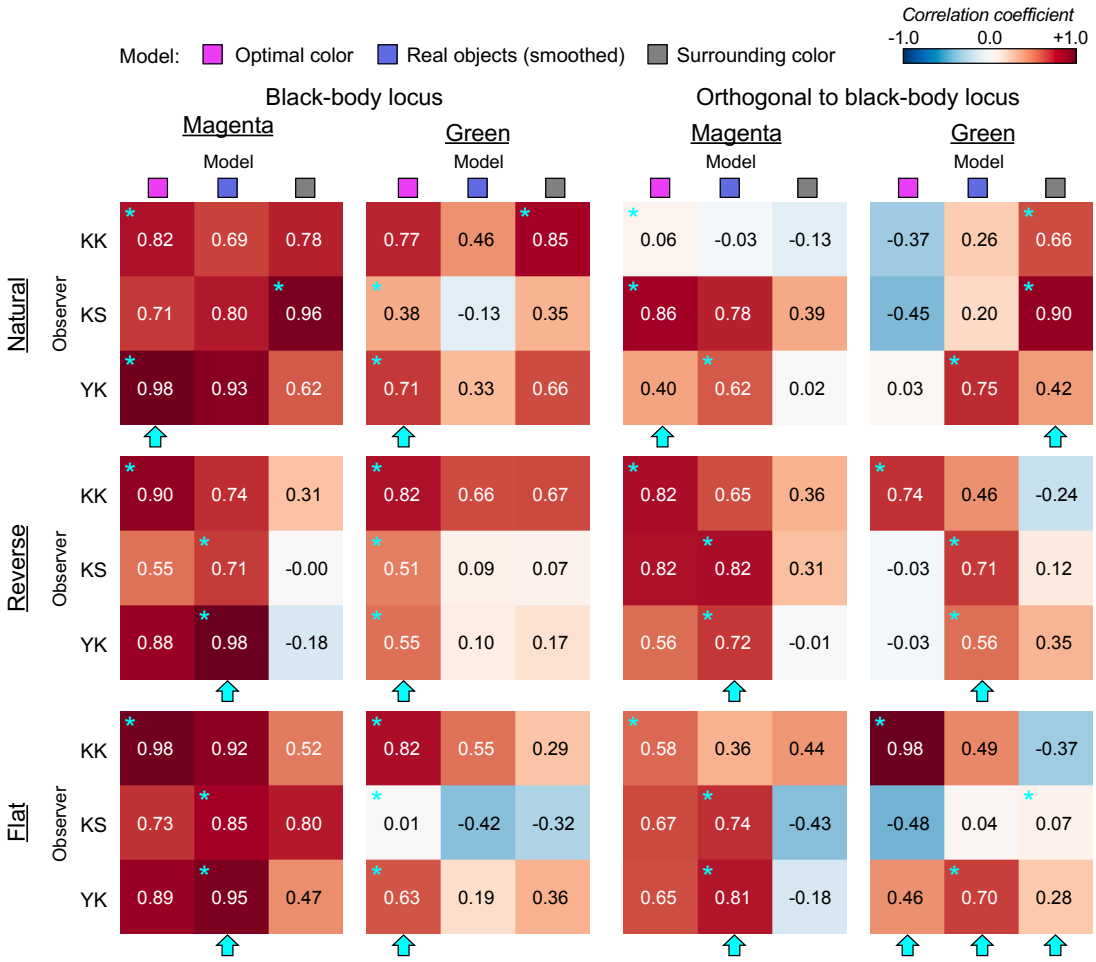

Figure 14: The matrices of Pearson's correlation coefficient calculated between observer settings and model prediction over 7 test chromaticities in Experiment 3. The cyan star symbol indicates the highest correlation coefficient across 3 models. The cyan arrows at the bottom of each subpanel show the model that received the highest number of cyan star mark.

In summary these results suggested that although the optimal color model and real object models can account for observer settings to some extent, overall coefficient values were substantially lower than those observed in Experiments 1 and 2. Also the surrounding color model showed good correlation in some cases. These results might imply that visual system does not have a rigid internal reference about upper-limit luminance under atypical illuminant and sometimes relies on external cues such as the color in surrounding stimuli. This trend was particularly true when the test chromaticities are sampled from the locus orthogonal to black-body locus.

Finally, we summarize correlation coefficient from three experiments to test whether correlation coefficient of optimal color model is higher for typical illuminants (Experiments 1 and 2) than atypical illuminants (Experiment 3). For each observer, we averaged correlation coefficient of optimal color model for all conditions in Experiment 1 and 2 (14 conditions), which serves as a summary statistic for a typical illuminant. For 20000K condition in Experiment 2, we used correlation coefficient value of the optimal color model under estimated illuminant as it predicted observer settings substantially better than the model under the ground-truth illuminant. We also calculated average correlation coefficient for all conditions in Experiment 3 (8 conditions). Then, the averaged correlation coefficients across all observers were 0.879 ± 0.0114 (average ± S.D.) for typical illuminant and 0.525 ± 0.155 for atypical illuminant. Welch's t-test (one-tailed, no assumption about equal variance) showed that optimal color model has a significantly higher correlation for typical illuminant than atypical illuminant ($t(2.01) = 3.94$, $p = 0.0290$). Also we performed the same analysis using correlation coefficient for the real object model which showed the same trend ($t(2.84) = 2.93$, $p = 0.0326$).

These results are consistent with the idea that human observers empirically learn the upper-limit luminance through observing colors in natural environments and use the criterion to judge whether a given surface is self-luminous or not. Since magenta and green illuminants are uncommon in natural environments, the visual system does not know the upper limit of surface colors under those illuminants. This interpretation may explain why prediction from optimal color model and real objects model did not well explain observers' luminosity thresholds in Experiment 3.

5. General Discussion

This study investigated potential determinants of luminosity thresholds. Three experiments showed that loci of luminosity thresholds are mountain-like shape peaking around the illuminant color and decreases as stimulus purity increases, which showed a strikingly similarity to the optimal color and real object loci. A simple alternative strategy which bases a judgement on a surrounding color distribution did not explain observers' settings well. Rather observers seem to hold an internal representation about at what luminance a surface should reach self-luminous. Moreover, such similarity between luminosity threshold and optimal-color/real-object loci was higher when surfaces are placed under illuminants along blue-yellow direction than magenta and green illuminants that are atypical in natural environments. These support an idea that visual system empirically internalizes the heuristic gamut of surface colors through an observation of colors in a daily life. Going back to the original question whether visual system relies on external or internal reference for luminous judgement, the present study strongly supports an internal reference hypothesis. However, in Experiment 2, the peak of the loci

of luminosity thresholds were strongly influence by the color temperature of illuminant lighting surrounding stimuli. Thus, though the surrounding color model implemented in this study did not explain observers' settings well, it should be noted that properties of external stimuli are also likely to influence luminosity thresholds.

Color constancy is often described as a visual ability to identify a surface under different illuminants. A surface reflects a light, and the reflected light enters our eyes. Because the reflected light is a product of surface and illuminant components, color constancy is often framed as a process in which our visual system estimates the influence of illuminant. The "brightest is white" heuristics, which assumes that a surface with the highest luminance provides the closest information about the illuminant color, has been known as an influential approach to estimate an illuminant color (Land, 1977). However, self-luminous objects do not carry information about scene illuminant, which might cause an misestimation of illuminant if included in a scene. In general, when we received an intense light from a surface, there are two ways to interpret this. One is that the surface is placed under an intense illuminant and the other is that the surface is self-luminous. This example highlights that generation of luminous percept needs to be incorporated into a process of color constancy. In fact, Fukuda & Uchikawa (2014) showed that a surface appearing in aperture-color mode does not have a strong influence on observers' estimates of illuminant.

We chose a set of colored circles as experimental stimuli to directly test our hypothesis while excluding any other cues. However, it is reported that changing a material property could affect the mode of color appearance (Kuriki, 2015). Also, our experimental stimuli

were simulated to be uniformly illuminated by a single illuminant, but in natural environments the spectra hitting an object surface changes from one direction to another (Morimoto et al., 2019). The presence of multiple illuminants means that we need to consider multiple optimal color distributions, and thus loci of luminosity thresholds measured under such environment might also change. Despite a growing amount of research on material perception (Fleming, 2013), luminous perception is little studied in the field. While our choice of stimuli was necessary for experimental control, it will be interesting whether our finding applied a wider range of stimuli that have complex material properties and are illuminated in non-uniform ways.

One closely related phenomenon to self-luminous perception would be brightness perception of colored objects. The Helmholtz-Kohlrausch effect describes that stimuli with high purity appear to have high brightness even if luminance was kept the same. There are reports that the effect is observed under a variety of viewing conditions (Nayatani et al., 1991; Donoforio, 2011). However it has been uncertain why a color with high purity needs to appear brighter. Curiously, as observed in the present study the same trends hold for luminosity thresholds, a surface with high purity reaches the limit of surface color mode at lower luminance level. Thus, if we take a strategy to determine the brightness of colored stimuli in comparison to the theoretical upper-limit luminance at the chromaticity we could account for why the Helmholtz-Kohlrausch effect exists. Uchikawa et al. (2001) directly focused on this relationship and argued that saturated colors appear brighter because visual system knows that it has a lower limit and brightness might be determined in proportion to the theoretical upper-limit luminance.

Identifying the range of natural colors has been one major focus especially in the field of color science (Pointer, 1980). While the limit of chromaticity has been well characterized, little is known regarding the luminance limit. In this study, we used SOCS reflectance dataset as a reference to draw an upper-luminance boundary for real objects. The database covers a wide range of color space as it includes man-made materials such as ink which can have narrow-band reflectances. We do not intend to claim that SOCS dataset in any sense represents all plausible natural reflectance spectra. Yet, our separate analysis based on 16 hyperspectral images (Nascimento, 2002, Foster 2006) showed that colors in those images were mostly covered in the gamut of SOCS dataset. Also, to our knowledge we have not encountered other dataset that has a larger color gamut than SOCS dataset. We also found that if we restrict samples to natural objects, the color gamut largely shrinks (see Figure 2 (b) in Morimoto 2016) and upper-limit luminance estimated from such sample would not predict obtained luminosity thresholds in this study. Also, in this study, we used a smoothed upper-limit luminance. If we instead use a raw unsmoothed data, the correlation coefficient lowered in almost all tested conditions. These results show that a precise evaluation of the abundance of reflectance samples in real world seems to play a key role in understanding the luminosity percept. When more reflectance datasets become available in future, the gamut of real objects should be re-evaluated.

In summary, our results suggested that there is a mysterious relationship between luminosity threshold and optimal colors. Yet it is difficult to make a conclusive statement as to whether the optimal color model is better in accounting for luminosity thresholds than real object model. This is partially because the optimal color locus well resembles

the locus of real objects, leading to high correlation between predictions from two models. Furthermore, an intrinsically more challenging question would be that how our visual system learns the optimal color locus even though optimal colors do not exist in the real world. Considering this point, one plausible theory would be that our visual system empirically learns natural color distributions through seeing colors in a daily life and develops the heuristic gamut of surface colors. Then, a given surface appears self-luminous when its luminance exceeds this heuristic upper-limit luminance. As argued above, SOCS dataset does not fully represent all real reflectance that can exist, and it is possible that the real gamut is larger than our estimation. As we have more surfaces, the gamut of surface color expands, and in theory it will eventually converge to the optimal color distribution. There is a report that Japanese monkeys (Macaca fuscata) raised only under monochromatic light do not develop color constancy (Sugita, 2004). Our current study also presents a potential link between our perceptual judgment and importance of learning natural scene statistics available in the real world.

Supplementary Material

Figure S1 shows individual observer settings in Experiment 2. There are some individual variations but overall trend was similar across individuals.

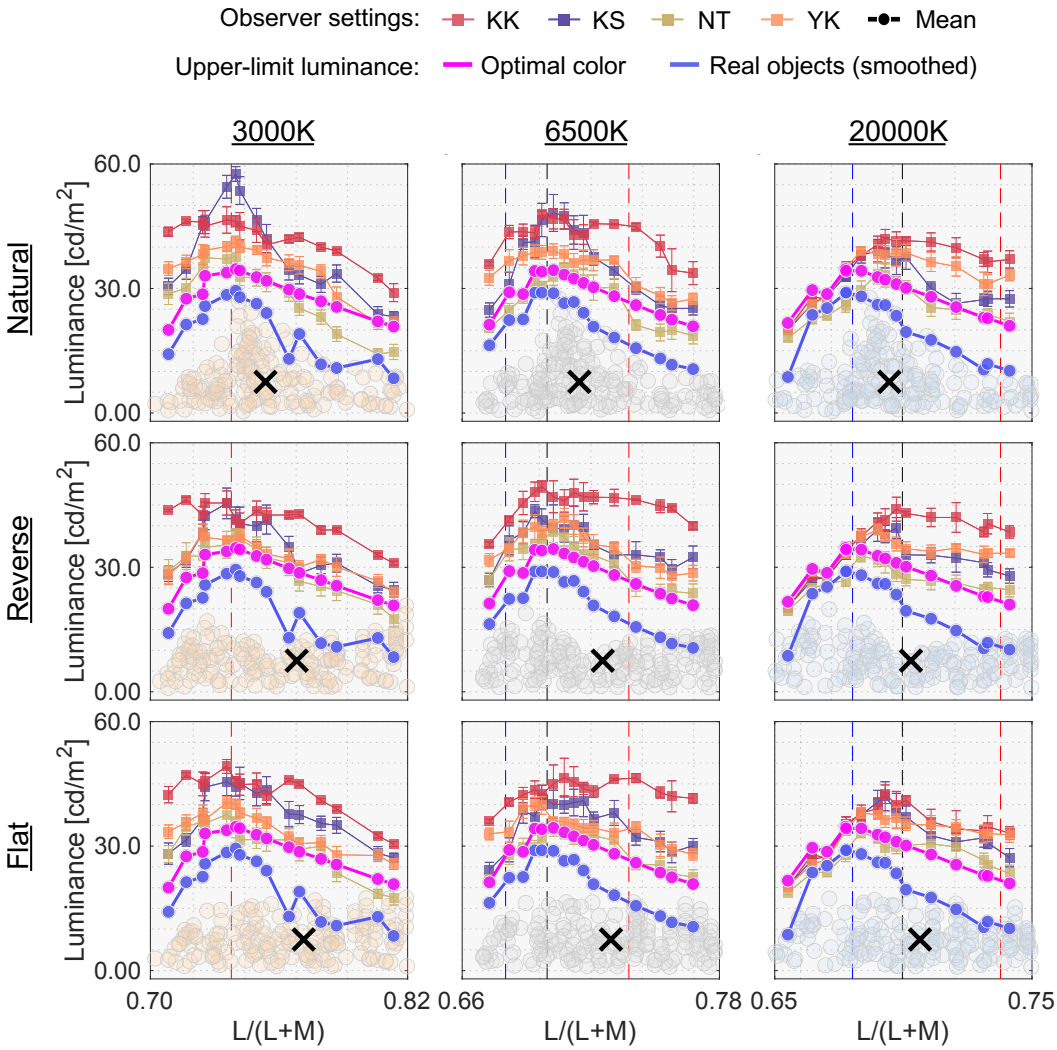

Figure S1: Individual observer settings in Experiment 2. Colored square symbols indicate averaged setting across 10 repetitions for each observer. The error bar indicates ± S.E across 10 repetitions. The magenta circle symbols denote the optimal color locus and the blue line shows the real objects locus. The vertical dashed line shows the chromaticity of the test illuminant. The black cross symbol indicates mean LMS value across surrounding stimuli. Notice that the horizontal range differs across panels.

Acknowledgement

This work was supported by JSPS KAKENHI Grant Number JP19K22881, JP17K04503 and 26780413. TM is supported by a Sir Henry Wellcome Postdoctoral Fellowship awarded from the Wellcome Trust (218657/Z/19/Z) and Junior Research Fellowship from Pembroke College, University of Oxford.

Data access

The raw experimental data will be available at a data repository. Codes to reproduce figures will be available at https://github.com/takuma929 at the time of publication.

Reference

Bonato F, Gilchrist AL. (1994). The Perception of Luminosity on Different Backgrounds and in Different Illuminations. Perception. 23, 9, 991-1006.

Bonato, F., Gilchrist, A.L. (1999). Perceived area and the luminosity threshold. Perception & Psychophysics, 61, 786–797.

Brainard. D. H. (1998). Color constancy in the nearly natural image 2 Achromatic loci. Journal of the Optical Society of America A, 15, 2, 307–325.

Brown, R. Background and illuminants: the yin and yang of colour constancy. in Colour Perception: Mind and the Physical World, R. Mausfeld and D. Heyer, eds. (Oxford University, 2003), 247–272.

Buchsbaum, G. (1980). A spatial processor model for object colour perception. Journal of the Franklin Institute, 310, 1, 1–26.

Donofrio, R.L. (2011). Review Paper: The Helmholtz-Kohlrausch effect. Journal of the Society for Information Display, 19, 658-664.

Evans, R. M. (1959). Fluorescence and Gray Content of Surface Colors. J. Opt. Soc. Am. 49, 1049-1059

Evans, R. M. & Swenholt, B. K. (1967). Chromatic strength of colors: dominant wavelength and purity. J. Opt. Soc. Am. 58, 580-584. J. Opt. Soc. Am. 58, 580-584.

Evans, R. M. & Swenholt, B. K. (1968). Chromatic Strengths of Colors, Part II. The Munsell System. J. Opt. Soc. Am. 58, 580-584.

Evans, R. M. & Swenholt, B. K. (1969). Chromatic Strength of Colors, III. Chromatic Surrounds and Discussion. J. Opt. Soc. Am. 59, 628-634.

Fleming, R. W. (2013). Material Perception. Annual Review of Vision Science, 3, 365–388.

Fukuda, K. & Uchikawa, K. (2014). Color constancy in a scene with bright colors that do not have a fully natural surface appearance. Journal of the Optical Society of America A, 31, 4, A239–A246.

Gilchrist, A. & Bonato, F. (1995). Anchoring of lightness values in center-surround displays. Journal of Experimental Psychology: Human Perception and Performance, 21, 6, 1427-1440.

Gilchrist, A., Kossyfidis, C., Bonato, F., Agostini, T., Cataliotti, J., Li, X., Spehar, B., Annan, V. & Economou, E. (1999). An anchoring theory of lightness perception. Psychological Review, 106, 795–834.

Judd, D. B., MacAdam, D. L. Wyszecki, G., Budde, H. W., Condit, H. R., Henderson S. T., and Simonds J. L. (1964) “Spectral distribution of typical daylight as a function of correlated color temperature,” J. Opt. Soc. Am. 54(8), 1031–1040

Kuriki, I. (2015) Effect of material perception on mode of color appearance. Journal of Vision, 15(8), 4.

Krinov, E. (1947) Spectral reflectance properties of natural formations. Tech. rep., National Research Council of Canada. Technical Translation: TT-439.

Land, E. H. (1977). The Retinex Theory of Color Vision, Scientific American, 237, 6, 108 -128.

Long, F., & Purves, D. (2003) Natural scene statistics as the universal basis of color context effects. Proceedings of the National Academy of Sciences, 100, 25, 15190-15193.

Lotto, R. B. & Purves, D. (2000) An empirical explanation of color contrast. Proceedings of the National Academy of Sciences, 97, 23, 12834-12839.

MacAdam, D. (1935a). The theory of the maximum visual efficiency of colored materials. Journal of the Optical Society of America A, 25, 249–252.

MacAdam, D. (1935b). Maximum visual efficiency of colored materials. Journal of the Optical Society of America A, 25, 361–367.

MacLeod, D. I. A., & Boynton, R. M. (1979) Chromaticity diagram showing cone excitation by stimuli of equal luminance. Journal of the Optical Society of America A, 69, 1183–1186.

Maloney, L. T. & Wandell, B. A. (1986) Color constancy: a method for recovering surface spectral reflectance Journal of the Optical Society of America A, 3, 1, 29–33.

Morimoto, T., Fukuda, K., & Uchikawa, K. (2016) “Effects of surrounding stimulus properties on color constancy based on luminance balance”, Journal of the Optical Society of America A, 33, 3, A214–A227.

Morimoto, T., Kishigami, S., Linhares, J. M. M., Nascimento, S. M. C., & Smithson, H. E. (2019). Hyperspectral environmental illumination maps: characterizing directional spectral variation in natural environments. Optics Express, 27, 32277-32293.

Morimoto, T., Kishigami, S., Linhares, J. M. M., Nascimento, S. M. C., & Smithson, H. E. (2021). Human color constancy based on the geometry of color distributions. Journal of Vision, 27, 21(3):7. doi: https://doi.org/10.1167/jov.21.3.7.

Nascimento, S.M.C., Ferreira, F.P., & Foster, D.H. (2002). Statistics of spatial cone-

excitation ratios in natural scenes. Journal of the Optical Society of America A, 19, 1484-1490.

Foster, D.H., Amano, K., Nascimento, S.M.C., & Foster, M.J. (2006). Frequency of metamerism in natural scenes. Journal of the Optical Society of America A, 23, 2359-2372.

Nayatani Y., Umemura, Y., Sobagaki, H., Takahama, K. & Hashimoto, K. (1991). Lightness perception of chromatic object colors. Color research and application, 16, 1.

Pointer, M. R. (1980) The gamut of real surface colours. Col. Res. Appl. 5, 145–155.

Speigle, J. M. & Brainard, D. H. (1996). Luminosity thresholds: effects of test chromaticity and ambient illumination. Journal of the Optical Society of America A, 13, 436-451

Stockman, A. and Sharpe, L. T. (2000) The spectral sensitivities of the middle- and long-wavelength-sensitive cones derived from measurements in observers of known genotype. Vision Research, 40, 1711–1737.

Sugita, Y. (2004). Experience in Early Infancy Is Indispensable for Color Perception. Current Biology, 14, 3, 1267- 1271.

Uchikawa, K., Koida, K., Meguro, T., Yamauchi Y., & Kuriki, I. (2001). Brightness, not luminance, determines transition from the surface-color to the aperture-color mode for colored lights. Journal of the Optical Society of America A, 18, 737–746.

Uchikawa, H., Uchikawa, H. & Boynton, R. M. (1989). Influence of achromatic surrounds on categorical perception of surface colors. Journal of the Optical Society of America A, 29, 7, 881–890.

Uchikawa, K., Fukuda, K., Kitazawa, Y., & MacLeod, D. I. A. (2012). Estimating illuminant color based on luminance balance of surfaces. Journal of the Optical Society of America A, 29, 2, A133–A143.

Ullman, S. (1976) On visual detection of light sources. Biological Cybernetics, 21, 205–211.

Yamauchi, Y. & Uchikawa, K. (2005). Depth information affects judgment of the surface-color mode appearance. Journal of Vision, 5, 515-524.